



## Spectrometer for Marine Litter

### ***ESR - Executive Summary Report***

ESA contract no. 4000129488/19/NL/BJ/ig

EUROPEAN SPACE AGENCY  
CONTRACT REPORT

The work described in this report was done under ESA contract.  
Responsibility for the contents resides in the author or organisation that prepared it.

	Name	Company or Institute	Signature
Prepared by	Hugo Silva	INESC TEC	
	Diana Viegas		
	Sara Freitas		
	Pedro Jorge		
Reviewed by	Eduardo Silva	INESC TEC	
Distribution list	Paolo Corradi, TEC-MMO	ESA/ESTEC	

EUROPEAN SPACE AGENCY  
CONTRACT REPORT

The work described in this report was done under ESA contract.  
Responsibility for the contents resides in the author or organisation that prepared it.

## Table of Contents

1	Background .....	1
2	Laboratory Characterization of Marine Litter .....	4
3	Airborne Campaigns.....	7
3.1	Artificial Target Assembly .....	8
3.2	Hyperspectral Image Acquisition Setup .....	8
3.3	Flight Campaigns .....	9
4	Results .....	9
5	Conclusions.....	14

# 1 Background

Marine Litter is currently a global threat to marine ecosystems, large quantities of marine litter and debris are drifting and accumulating in the oceans, as well as polluting rivers, beaches, and coastal areas. Even though marine litter has been already identified by key stakeholders as a problem that needs to be tackled, there is still lot of work to be conducted in different domains to diminish the amount of marine litter that ends up in the water.

Monitoring marine litter is very important in view to identify the sources, the sinks and the trend of the pollution manifestations and act accordingly. However, the current ground data collection approaches are limited both in terms of spatial and temporal resolution. Remote sensing (including airborne and orbital) systems have the potentiality to cover larger areas in a more systematic and periodic manner.

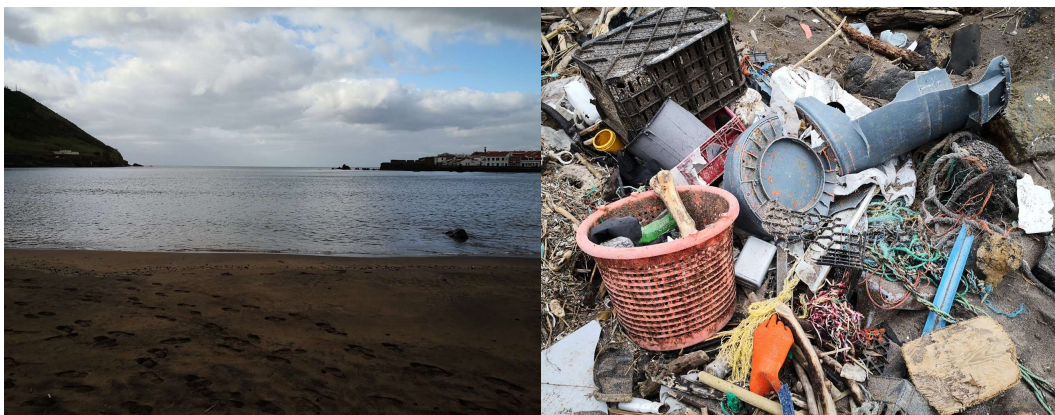


Figure 1 - Pim Bay Azores (left) image. Samples of marine litter concentration found at Pim Bay beach (right) image

Currently, marine litter characterization is performed on ground by taking into consideration the plastics characteristics such as type and size. This taxonomy was proposed by the UK Marine Conservation Society and adopted by most scientific communities, as described and is displayed Veiga et al.<sup>1</sup> in Table 1.

Table 1 – Compilation of the main types of plastic<sup>1</sup>

Types of litter	Main source
Public litter	Items dropped or left by the public on the coast or inland and carried by winds and rivers
Fishing litter	Includes commercial and recreational items (such as fishing line, nets, rope, weights and buoys)
Sewage Related Debris	Items flushed down the toilet such as cotton bud sticks, tampons and panty liners
Shipping	Items dropped or lost from ships
Fly tipped	Illegal disposal of waste including furnishings, pottery and ceramics
Medical	Includes anything medical such as inhalers, plasters, syringes
Non-sourced	Items too small or damaged to identify or not obviously attributable to a given source

The taxonomy covers the type of litter and the point of origin. However, scientists also use the plastics size as an attribute to classify individual marine litter samples. Normally, most authors adopt the size division described in Table 2 to classify plastics concerning their size interval from microplastics (<1mm) to macroplastics samples (>25mm).

1. Veiga, J.; Fleet, D.; Kinsey, S.; Nilsson, P.; Vlachogianni, T.; Werner, S.; Galgani, F.; Thompson, R.; Dagevos, J.; Gago, J.; Sobral, P.; Cronin, R. *Identifying sources of marine litter*; 2016; p. 41. doi:10.2788/018068.

Table 2 - Plastics class depending on the size of the sample.

Denomination	Size
Small Microplastic	<1 mm
Large Microplastic	1.5 - 5 mm
Mesoplastic	5.1 - 25 mm
Macroplastic	>25 mm

To better study the source and geographic origin of the marine litter found in the ocean<sup>2</sup>, a Matrix Scoring Index technique was proposed that also classified marine litter samples based on the origin, means of release, pathway, and transport mechanism, as can be seen in Table 3 as example for marine litter found on the Northern Coast of Germany.

Table 3 - Some of the main plastic sources as well as their means of release, geographic origin, pathway, and transport mechanism for a few marine litter items found on the Northern coast of Germany.

	Source	Means of release	Geographic origin	Pathway	Transport mechanism
<b>Cotton bud sticks</b>	Consumers/ General public	Improper disposal down the toilet	Households	Sewage systems and/or rivers	Sewage, rivers, ocean currents and tides
<b>Plastic bags</b>	Coastal tourism & recreation	Littering (e.g. on beach)	Local (e.g. coastal town or beach nearby)	Direct entry (if at beach) or e.g. windblown (if town nearby)	Winds and tides
	Consumers/ General public	Littering (e.g. on street, from car, in natural area)	e.g. Distant (inland town)	Distant - Wind (blown) and/or rivers	Wind, rivers, ocean current and tides
	Waste management at beach	Overflowing open bin	Beach	Direct input	Wind, tides and currents
<b>Nets and pieces of nets</b>	Fisheries	Discard or unintentional loss overboard during net repair work at sea	E.g. Local fisheries, regional fisheries or distant fisheries	Direct entry nets get washed or thrown overboard	Winds (drift), currents and tides
	Fisheries	Loss of nets and pieces of net during fishing (snagging)	E.g. Local fisheries, regional fisheries or distant fisheries	Direct entry nets get snagged on wrecks, rocks etc. ripped off pieces of net remain attached to objects underwater or are released into the water column (ghost nets)	Winds (drift), currents and tides
	Fisheries and/or harbours	Discard or unintentional loss during net repair work on land or/and runoff from harbours	E.g. local fishing harbours	Direct entry nets washed, blown or thrown (swept) into harbour basins and washed out to sea	Winds (blow-off), tides and currents
<b>Injection gun cartridge (grease)</b>	Shipping including fisheries	Discard or unintentional loss overboard at sea local	Local (cartridges recorded on beaches are not fouled, not battered)	Direct entry from ships at sea	Winds (drift), currents and tides
<b>Tahitians (plastic sheeting to protect mussel cultures)</b>	Aquaculture	Unintentional loss or discard after use	Distant – International - Northwest France/Atlantic coast of France	Direct input	Winds, currents and tides

<sup>2</sup> Tudor, D.; Williams, A. Development of a "Matrix Scoring Technique" to determine litter sources at a Bristol Channel beach. Journal of Coastal Conservation 2004, pp. 119–127.

Another important aspect that marine scientists take into consideration when analyzing marine litter samples is the overall conditions of the sample, if it contains biofouling, and the wear and tear caused by the UV radiation among other factors.

Biofouling comprises the accumulation of microorganisms, plants, algae, or other small and similar organisms. This process reduces the buoyancy of plastic particles that sink below the sea surface. It has been found that small plastic items start to sink sooner than larger plastic items, due to the relation of buoyancy with item volume, while fouling is related to surface area, and small items have high surface area to volume ratios<sup>3</sup>.

Marine litter sources are also related to some natural disasters, such as the Japan tsunami on March 11, 2011. The tsunami triggered the dispersion of approximately 1.5 million tons of debris that ended up floating in an area that is scattered through the Pacific Ocean from North America to Hawaii.

Characterization of the reflectance spectra of plastic marine litter has been performed *in-situ*, in laboratories and on field. Garaba et al.<sup>4</sup> reported absorption features at the wavelengths from 905 to 955 (nm), 1160 to 1260 (nm), 1380 to 1480 (nm), and 1715 to 1750 (nm), and some minor absorption features in the bands 1030 to 1070 nm, 1510 to 1550 nm, 2000 to 2050 (nm) and 2300 to 2350 nm. To distinguish between the several types of plastics, the authors obtained band depth indexes in the following absorption features: 931, 1215, 1417 and 1732 (nm). They were also able to show that the possibility of detection of different features of absorption will depend on the plastic concentration and if they are wet or dry and from their submersion degree in the water. The question of being dry or wet affects mainly the spectrum intensity, which can make it more difficult to distinguish. They also reported a reduction of median band depth index for wet compared to dry plastics of 75%, 55% and 71% for 931, 1215 and 1732 nm, respectively.

The above-mentioned information is compiled in Figure 2, where it is possible to observe the main absorption features for five different types of plastics: PET, LDPE, PP, PVC and PS. The selection of these types of plastics is related to their abundance in the maritime environment.

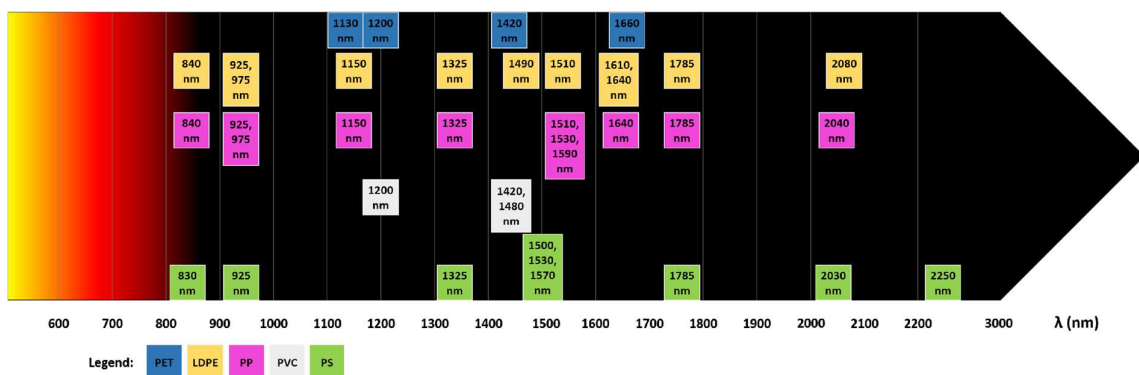


Figure 2 - Main Absorption Features for PET, LDPE, PP, PVS and PS plastic types.

In the project here presented, the objectives were: a) to enhance the findings of previous research work in the *in-situ* characterization of marine litter samples from the Porto Pim Bay in Azores by using different sensors and measuring devices; b) to conduct an airborne campaign to acquire a dataset of hyperspectral images of plastic targets on the sea and the coast; and c) to develop automated data processing tools to perform detection of plastic in the acquired hyperspectral images.

<sup>3</sup> Ryan, P. Does size and buoyancy affect the long-distance transport of floating debris? Environmental Research Letters 2015.

<sup>4</sup> Garaba, S.P.; Dierssen, H.M. An airborne remote sensing case study of synthetic hydrocarbon detection using short wave infrared absorption features identified from marine-harvested macro- and microplastics. Remote Sensing of Environment 2018, 205, 224–235. doi:10.1016/j.rse.2017.11.023.

## 2 Laboratory Characterization of Marine Litter

Analyses of the composition of different samples of marine litter, collected from the sea in the test site at Porto Pim in Faial Island Azores, were conducted during the project. The samples that were collected are composed mainly by: Polyethylene terephthalate (PET), Polypropylene (PP), Polyvinyl chloride (PVC), Polystyrene (PS), Polyethylene (PE) and Low-density polyethylene (LDPE) materials. The analyses had also the aim to investigate the physical status and chemical characteristics of the samples in order to possibly assess what changes these marine harvested plastics underwent during years of wear and tear, either by water or by UV radiation emitted by the sun.

The analyses found the most promising absorption bands to identify the different plastic materials. Complementarily, information on molecular and elemental composition was extracted, to better understand the nature of the plastic material and its environmental driven modifications. The samples were physically sorted to perform the largest number of tests simultaneously.

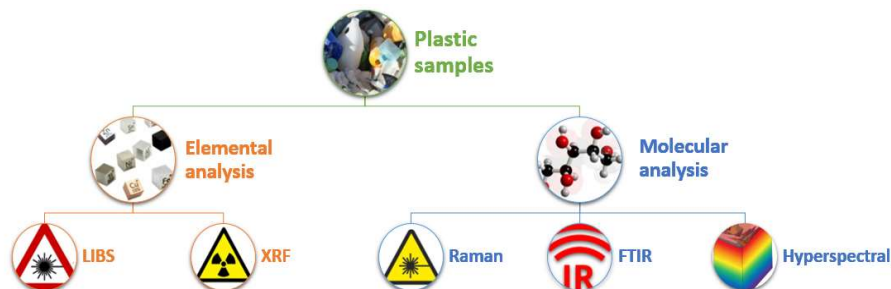


Figure 3 - Laboratory Marine Samples Characterization and Analysis

The samples were analyzed by using a set of techniques, suitable for either molecular or elemental analysis, namely Fourier-Transform Infra-Red (FTIR) Spectroscopy, Raman Spectroscopy, X-ray fluorescence (XRF), LASER-induced Breakdown Spectroscopy (LIBS) and Spectral radiance (UV-Vis-NIR)

These techniques were selected for their versatility and complementary features, which includes the ability to identify molecular bonds (FTIR and Raman), elemental composition (XRF and LIBS) and UV-VIS-NIR absorption bands (Spectral Radiance). Figure 4 to Figure 6 shows some of the results obtained with the different techniques.

Overall the analysis of the spectra obtained allowed to establish that the different materials were associated with distinctive spectral patterns. In addition to distinguishing the different types of plastic materials it was also possible to see clear changes on the spectrum when paint, biofilms and other overlays were present over the original plastic materials. This shows that, in addition to the element information that can be derived from the individual lines, simple classification schemes such as Principal Component Analysis (PCA) may be used to extract information on the type of material and its degree of transformation or environmental wear.



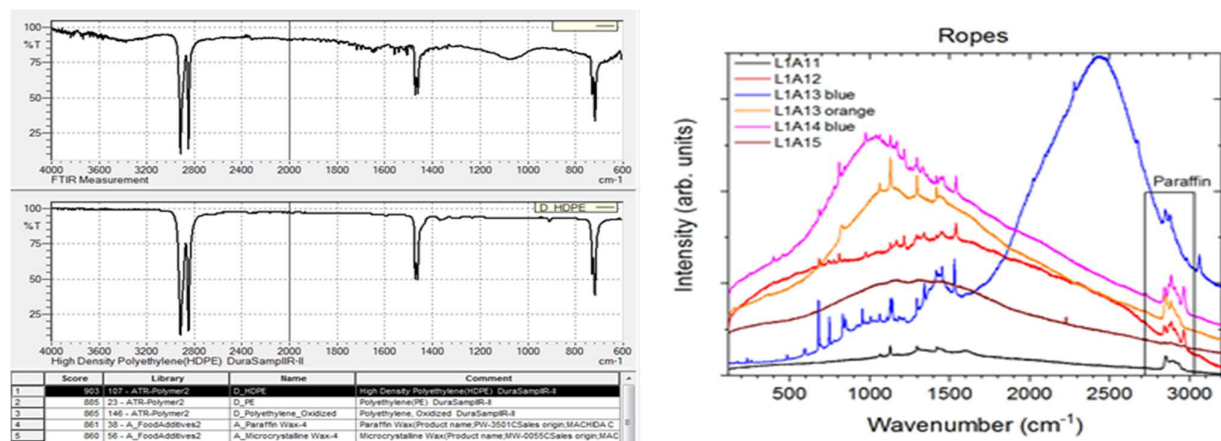


Figure 4 . FTIR (left) and Raman (right) plastic characterization spectra

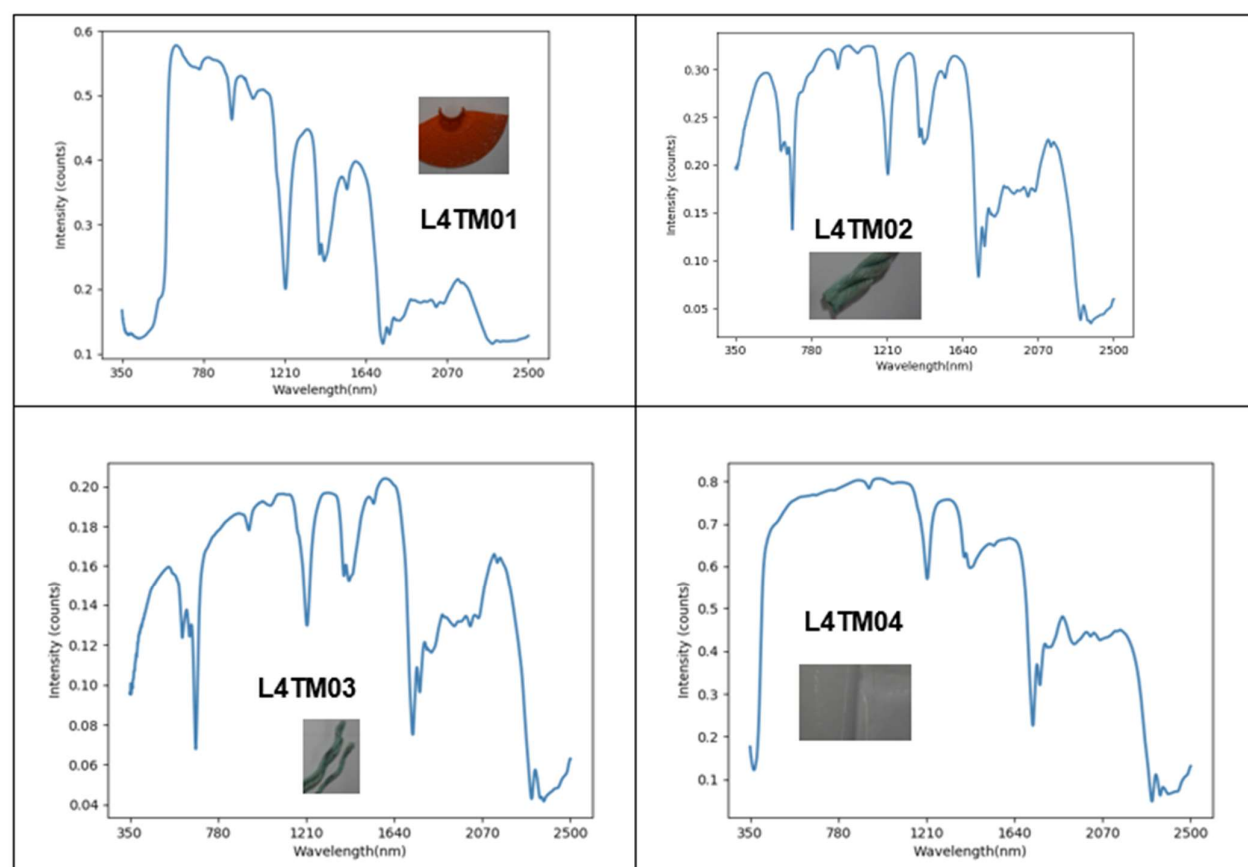
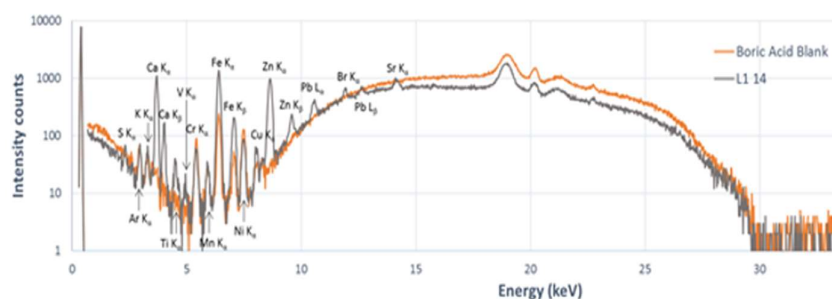
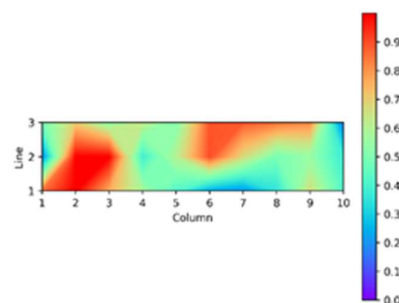


Figure 5 – Spectral Radiance (UV-Vis-NIR) of the collected plastic samples

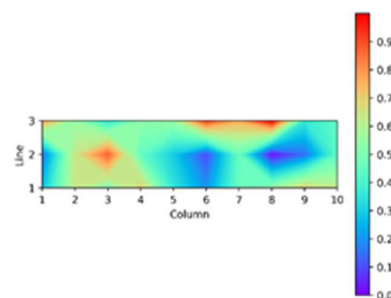
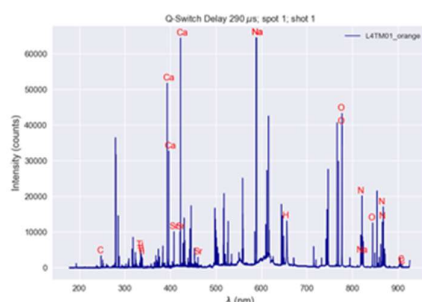




	Sample Name	Elements shown in sample and blank	Elements exclusive of sample
Lot 1	Sample A14	Ar, K, Cr, Mn, Fe, Ni, Cu	S, Ca, Ti, V, Zn, Pb, Br, Sr
Lot 2	Sample A05	Ar, K, Cr, Mn, Fe, Ni, Cu	S, Ca, Ti, Zn
Lot 2	Sample A12B	Ar, K, Cr, Mn, Fe, Ni, Cu	P, S, Ca, Ti



**Map of Calcium**



**Map of Copper**

*Figure 6 – XRF (top) and LIBS (bottom) characterization spectra*

The results from the local spectral radiance measurements allowed us to observe the main absorption bands, due to the plastic composition (mostly in the NIR) or from its coloration (VIS). These constitute good reference measurements for the in-flight spectral measurements, and allow to perceive the intrinsic bands of each material, without any environmental interference. Overall a good match was observed between the local and the in-flight spectral measurements. A more detailed analysis should be performed to understand the nature of the minute differences observed (atmospheric interference, instrumental response, etc).

FTIR analysis allowed for a relatively straightforward identification of the main plastic materials as there are available extensive databases with main molecular bonds. Therefore, this technique constitutes a very good reference, allowing to establish a correlation between main UV-VIS-NIR absorption bands and plastic composition.

Raman results produced similar results which were however plagued with intrinsic fluorescence of the samples, most probably originating from organic bonds. No relevant information was retrieved as compared with FTIR. Raman spatial resolution, nevertheless, may be useful when used in combination with LIBS surface mapping, allowing a composition mapping.

XRF was shown to have the ability to detect several elements, in particular metallic species and heavy species such as Pb and Cr. Overall, XRF measurements can constitute an interesting tool for local analysis allowing to obtain insight over which elements are aggregated to the plastic samples either from original pigments or which are later aggregated from the environment. When tested against the virgin materials it can also allow us to understand if some of these elements are being leached out to the environment.

Finally, LIBS has demonstrated the ability to detect the main elements of the material composition, such as C and H, as well as additional elements from pigments (Cu) or originating from the environment (Ca and Na). The ability of mapping the distribution of these elements over the surface of the sample, or through its depth was also verified. Such ability gives important insights on the distribution of the atomic species, allowing us to understand the degree of contamination or leaching from or to the environment.

In LIBS as in some of the other techniques, the amount of data collected is relatively large. The results here presented constitute a preliminary analysis of capabilities that can be explored in much more detail. Indeed, the use of signal processing and analysis tools when coupled with most of these techniques will allow retrieval of more detailed and consistent data. In particular, in the case of LIBS, in-house developed algorithms are being used to enable the identification and even quantification of trace elements, difficult to extract with traditional methods.

Overall, it was verified the complementarity of the different techniques, which, when used in combination, provide a much more complete insight on the properties of plastic debris scattered in the ocean. In particular, in addition to its original plastic matrix, it allows us to understand which kind of atomic species are associated with different materials, and/or different regions of the globe. This information is critical as it enables a more complete awareness of the environmental impact of these materials. Since most of these techniques are compatible and available with portable or transportable equipment, it can be envisioned an ideal scenario where large amounts of debris are probed locally, and correlated with remote sensing information. With large amounts of data, big data techniques can then be applied which eventually will provide a more complete awareness of the problem we are facing.

### 3 Airborne Campaigns

The project dataset campaign occurred in Faial Island Azores from the 16th until the 25th of September of 2020. The artificial target setups were placed in the Pim Bay area. Two different airborne setups holding a dual hyperspectral image equipment were used, consisting of two hyperspectral cameras that were able to acquire spectral information from 400nm to 2500nm wavelength. In Figure 7, it is possible to see the hyperspectral instrumentation on-board each platform. The first is a Cessna F150L, from Torres Vedras Aeroclub. The second one on the right image is a Grifo-X unmanned aircraft developed at the Centre for Robotics and Autonomous Systems of INESCITEC.



*Figure 7 - Manned Piloted Aircraft with the hyperspectral cameras on the landing gear, and Grifo-X UAV equipped with the hyperspectral cameras on the landing platform*

### 3.1 Artificial Target Assembly

Three different targets (100 m<sup>2</sup> each) were built for the field tests in Pim Bay, see Figure 8. Each target is composed of modular squares (2.5x2.5 m) made of threaded PVC tubing (2.5cm diameter). The targets were filled with different types of plastic debris: (1) low density polyethylene (previously used oyster spat collectors); (2) nets and ropes; (3) PET Plastic film.



*Figure 8 - Artificial Targets 10x10(m) Pim Bay Azores*

### 3.2 Hyperspectral Image Acquisition Setup

Concerning the equipment carried on-board each of the airborne platforms, it consisted of a system composed of two hyperspectral cameras, a CPU unit, GPS, and inertial system. One of the hyperspectral cameras was a Specim FX10e, a GIGe camera with a spectral range from 400 to 1000 nm wavelength and a spatial resolution of 1024 pixels. The other camera was a HySpex Mjolnir S-620, a hyperspectral system composed by the hyperspectral camera, a data acquisition unit, GPS, dedicated inertial system and a RGB camera, integrated into the same closed box. This hyperspectral camera has 620 pixels of spatial resolution and covers a spectral range from 1000 to 2500 nm wavelength.

The HySpex Mjolnir S-620 also holds a controller board that is connected to the GPS/INS to synchronize an external trigger. One of the changes performed to the system was to use this signal to also trigger the SPECIM FX10e, which allowed synchronization of both cameras image acquisition, having the GPS/INS signal as global reference. In Figure 9 is possible to see an illustration of the payload scheme.

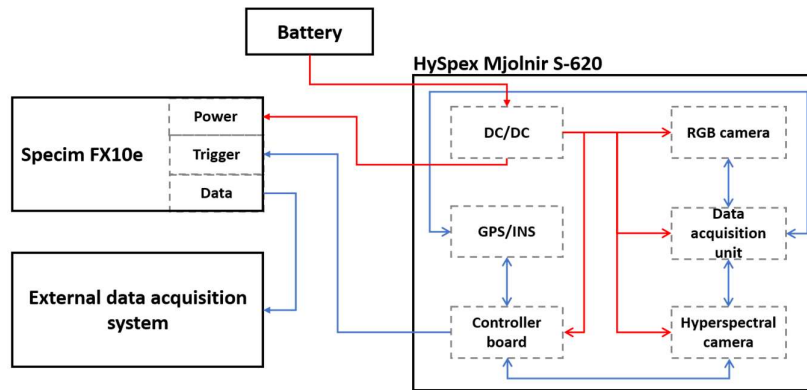


Figure 9 - Hyperspectral Image Payload Scheme

### 3.3 Flight Campaigns

Figure 10 shows the trajectory made by the aircraft and the drone onto the bay. The aircraft flew on three different days: 17/9, 18/9, and 20/9, and performed 4 flights during these days. Due to adverse atmospheric conditions, the aircraft did not fly on 19/9.

The drone flew on three different days: 22/9, 24/9, and 25/9, and performed 5 flights during these days. Due to adverse atmospheric conditions, the aircraft did not fly on 23/9.



Figure 10 - F-Buma (airplane left image) and X-Grifo (drone right image) flight trajectories over the artificial target locations Pim Bay Azores

## 4 Results

The characterization of the acquired hyperspectral imaging data is important. But to help solving the problem of marine litter detection and identification, automated means of detection need to be utilized to process large amounts of data.



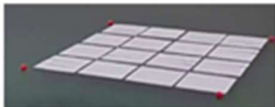
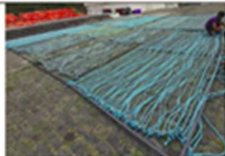
Therefore, we developed, trained, and compared the results of two machine learning (ML) algorithms that detect and classify marine litter samples, namely: Random Forest (RF) and Support Vector Machines (SVM). The algorithms were only tested in the F-BUMA acquired data, due to the time-consuming of manual annotating the dataset for ground-truth and training purposes.

The training of the model was performed with data collected during the F-BUMA 18/09/2020 flight, which was divided to be used for training and fine-tuning of the model parameters. The second flight, from 20/09/2020, was used for testing the results. This means that the model was trained using data from a different day than the one used for the prediction.



Given the data characteristics, the flights were divided into flybys over the target, and only the data in the target's vicinity was used for training and prediction. Table 5 and Table 6 show the pixel distribution for each class in each flyby. Class 1 represents the Orange target data, class 2 corresponds to the White target data, and class 3 the Rope target data. Class 0 was created with all the remaining pixels, containing both land and water data. It was necessary to create this class to train the methods to recognize the characteristics of the non-marine litter pixels, by grouping them all in one class. In Table 4 is possible to observe some examples of the class's components.

*Table 4 - Targets used during the dataset collection and their division between the classes*

Class 0 Water and Land (houses, trees, streets, cars, and others materials)	Class 1 Orange plastic target	Class 2 White plastic target	Class 3 Ropes target
			

*Table 5 - 18/9 F-BUMA flight data analysis, class 1 corresponds to the orange target data, class 2 to the white target, and class 3 to the rope target data. Class 0 was created with all the remaining pixels, containing both land and water data.*

flyby	Class 0	Class 1	Class 2	Class 3
0	57259	299	664	678
1	125732	399	857	732
2	86479	454	1203	1144
3	153180	462	1880	1338
4	51438	700	1182	0
5	138612	620	1658	1710
6	87266	696	1358	1200
7	117078	489	1373	1960

*Table 6 - 20/9 F-BUMA flight data analysis, class 1 corresponds to the orange target data, class 2 to the white target, and class 3 to the rope target data. Class 0 was created with all the remaining pixels, containing both land and water data.*

flyby	Class 0	Class 1	Class 2	Class 3
0	15604	516	0	0
1	29522	858	0	0
2	47986	662	671	281
3	72742	715	1157	1026
4	52024	626	670	0
5	94414	626	670	0
6	167177	1547	1682	2574
7	81713	813	864	930
8	183419	2640	1928	1733

To overcome some limitations in the training of the data, some training techniques were adopted in the experiments, namely:

- Class imbalance: As can be observed in Table 5 and Table 6, the number of pixels for each class has a huge variation. Some of the flybys do not hold information about all the classes, and the difference between the class 0 pixels and the other classes is significant. Therefore, we had randomly selected several samples so that the number of points is identical for each class. This was required, so the class with the highest number of points does not become dominant leading to overfitting;
- Feature normalization: Given the characteristics of the hyperspectral data that is affected by the variability of atmospheric conditions, particularly direct sunlight, it is necessary to carry out

its normalization. To perform this step, we used the sklearn python library pre-processing module, to normalize the feature data to unit variance.

- Given the characteristics of the flight (altitude), the targets will appear relatively small (resolution) in the datasets. In addition, there are targets that due to their physical construction, will have water in the middle, such as the orange (class 1) and rope targets (class 3). Furthermore, due to the size of targets in the final dataset, marking the ground truth to completely exclude the water in the middle of the target is very difficult. Therefore, it is still necessary to take this into account and try to balance this with the number of pixels provided to train the algorithm;
- The targets were always located in the same area. However, due to some variations in the flights mainly because of atmospheric conditions, there are flybys in which a considerable amount of land was observed. To allow the methods to learn the terrain characteristics, some land points were added to class 0. This land point contains data from houses, cars, ropes, trees, sand, and others objects. Due to this, the number of land pixels increased considerably, to ensure that, when selecting the points randomly, all these classes have some representation in class 0. This class is not a pure class (it does not contain only one type of material) but it is a class with a combination of dozens of materials that is not intended to be identified *per se*.

Considering all the aforementioned constraints the data was then processed for training. In this case, the number of pixels for ground-truth in each class was the following:

- Class 0: 170773 randomly selected pixels;
- Class 1: All the pixels contained in the training dataset, 4119 pixels;
- Class 2: 4119 randomly selected pixels;
- Class 3: 7000 randomly selected pixels;

The selection of the number of pixels for training each class was based on the maximum number of pixels present in the training data for class 1, since this was the class with fewer available pixels to identify. During the training process, we also had to add more class 3 pixels since it was difficult to manually select pure rope pixels.

Both RF and SVM methods implementation based on Python sklearn used the same training points from the 18/9 F-BUMA flight and the same test data from the 20/9 F-BUMA flight.

Both RF and SVM methods were trained with the training data from the 18/09/2020 flight. The aim was to create a model to be evaluated using the data collected during the 20/09/2020 flight, and Table 7 shows the prediction analysis for both algorithms (RF, SVM), using the following metrics: precision, recall, F1-score, and accuracy.

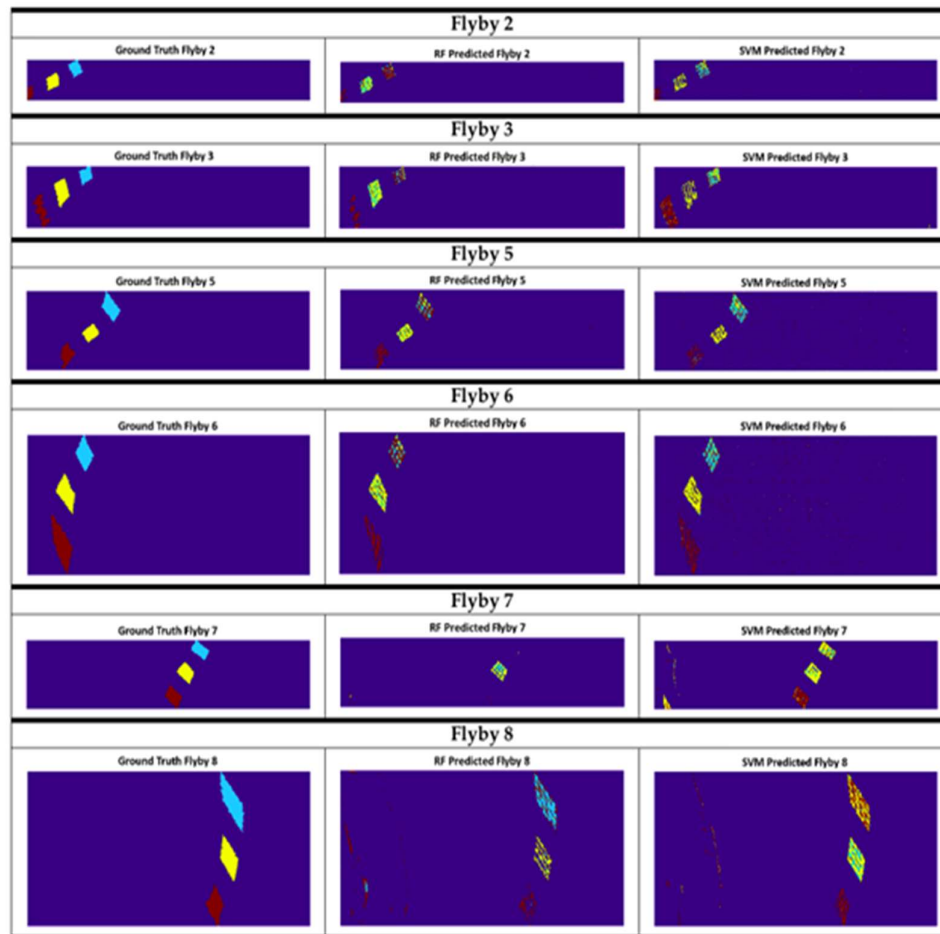
Table 7 - Results obtained for the test data (20/09/2020 flight) for random forest (RF) and support vector machine (SVM) algorithms.

Flyby 2								
	RF				SVM			
Class	Precision	Recall	F1-Score	Accuracy	Precision	Recall	F1-Score	Accuracy
0	0.99	1	0.99	97.35 %	0.99	0.99	0.99	97.47 %
1	0.24	0.12	0.16		0.75	0.42	0.54	
2	0.85	0.42	0.56		0.66	0.47	0.55	
3	0.18	0.44	0.26		0.22	0.50	0.31	
Flyby 3								
	RF				SVM			
Class	Precision	Recall	F1-Score	Accuracy	Precision	Recall	F1-Score	Accuracy
0	0.99	1	0.99	97.34 %	0.99	0.99	0.99	97.27 %
1	0.20	0.13	0.16		0.75	0.38	0.51	
2	0.85	0.53	0.65		0.56	0.43	0.49	
3	0.45	0.38	0.41		0.52	0.74	0.61	
Flyby 5								
	RF				SVM			
Class	Precision	Recall	F1-Score	Accuracy	Precision	Recall	F1-Score	Accuracy
0	0.99	1	0.99	98.09 %	0.99	0.99	0.99	97.06 %
1	0.71	0.25	0.37		0.77	0.46	0.58	
2	0.74	0.62	0.67		0.57	0.59	0.58	
3	0.38	0.56	0.45		0.21	0.47	0.29	
Flyby 6								
	RF				SVM			
Class	Precision	Recall	F1-Score	Accuracy	Precision	Recall	F1-Score	Accuracy
0	0.99	1	0.99	97.92 %	0.99	0.98	0.98	96.56 %
1	0.52	0.22	0.31		0.71	0.48	0.57	
2	0.85	0.59	0.70		0.78	0.67	0.72	
3	0.50	0.42	0.46		0.27	0.51	0.35	
Flyby 7								
	RF				SVM			
Class	Precision	Recall	F1-Score	Accuracy	Precision	Recall	F1-Score	Accuracy
0	0.98	1	0.99	97.32 %	1	0.99	0.99	98.01 %
1	0.01	0	0.01		0.50	0.16	0.24	
2	0.95	0.45	0.61		0.44	0.72	0.54	
3	0.17	0.01	0.02		0.64	0.76	0.70	
Flyby 8								
	RF				SVM			
Class	Precision	Recall	F1-Score	Accuracy	Precision	Recall	F1-Score	Accuracy
0	0.99	0.99	0.99	97.44 %	0.99	0.99	0.99	97.28 %
1	0.85	0.55	0.66		0.10	0.02	0.04	
2	0.94	0.36	0.52		0.46	0.55	0.50	
3	0.21	0.35	0.26		0.30	0.51	0.38	

Table 8 illustrates the detection and classification results compared with ground-truth information.



Table 8 - Figures showing the results obtained for the test data (20/09/2020 flight) for random forest(RF) and support vector machine (SVM) algorithms. In the first column are illustrated the ground-truth for each flyby, the second column shows the prediction made by the random forest algorithm, and the last column represents the predicted values by the support vector machine algorithm



The fact that the targets have 10x10 meters dimensions composed of 4x4 squares each one with 2.5x2.5 meters, influenced negatively the results. Meaning that at 600 meters average flight altitude it is very difficult to manually annotate a ground-truth pixel as "pure". Therefore, there is no absolute way to be sure that the target pixel is not overly dominated by water. Even though the targets are still able to be identified in most of the flybys, the precision rate and the recall rate are not uniform for all three targets indicating that on some of those flybys the targets could be submerged in some areas. Which is something to be expected in real environment scenarios.

Concerning the implemented methods (RF, SVM), it is possible to see both from the aforementioned Table 7 and Table 8 that the SVM provides slightly more accurate results. The SVM can detect all three targets in all the flybys, but the precision and recall values vary between the flybys. RF provides more stable results when it detects a target but sometimes is unable to detect the targets, see flybys 7 and 8.

However, even with the SVM methods, the results show a non-uniform detection pattern, particularly in class 2. This is the case since the class 2 target is a more common plastic-type that can be found in structures of houses or agriculture making it easier to be detected outside the target areas. In flyby 7 and flyby 8 it is possible to identify anomalies in class 1 and class 2 results in the SVM method. Both flybys show the presence of "land" in the identification of the targets. Given that class 0 is not a water target related class but instead a "non-marine litter" class. This may suggest the appearance of unknown artifacts of class 0 that were wrongly classified as class 2 in flyby 7 and class 1 in flyby 8.

Overall the RF and SVM methods show potential to be able to detect marine litter i.e. plastic samples using hyperspectral imaging on-board an aircraft at a reasonable altitude 600 meters altitude, with 0.75-0.95 precision values and not many false positives. The model trained from previous flight days allowed to classify correctly most of the targets, the presence of submerged target pixels made it more difficult for the methods to classify all the target pixels correctly, as well as made extremely challenging the distinction between the different types of plastic that constituted each target.

## 5 Conclusions

The Spectrometer for Marine Litter project was a major step for the consortia and particularly for INESCTEC in the development of sensing & perception mechanisms for oceanic environment applications. This project is an interdisciplinary project that involved researchers with diverse backgrounds i.e., engineers, physicists, biologists, marine biologists. This is important because marine litter is a complex problem, and a comprehensive approach to the study and understanding of the phenomena as a whole is required.

Even though the project duration was limited and affected by delays and restrictions due to Covid-19, important knowledge was acquired in the field of remote sensing applications for marine litter detection, e.g. how information learned from in-situ measurements can be used in (spectral) databases to develop algorithms for novel remote sensing systems.

The results obtained in each project task provide answers to specific questions, e.g. remote acquisition system and spectral bands selection, but most of all indicate research pathways that can be further explored. We presented a detailed development plan with ideas that can be further developed taking into consideration the findings of the project.

The project also collected large amounts of data, that is being catalogued to be put to use for the remote sensing community and will be made available before the end of the year.